



Integral of Sporopollenin Autofluorescence Intensity (ISAI), a novel marker for UV adaptation in spores/pollen

Xin-Lei Jia^{1,2} , Xi-Long Wang¹, Yi-Yun Chen³, Li-Mi Mao³, Hui Shen⁴, Zhong-Nan Yang¹ , Ying Xiao^{2*} and Jing-Shi Xue^{1*}

¹ Shanghai Key Laboratory of Plant Molecular Sciences, College of Life Sciences, Shanghai Normal University, Shanghai 200234, China

² The SATCM Key Laboratory for New Resources & Quality Evaluation of Chinese Medicine, Institute of Chinese Materia Medica, Shanghai University of Traditional Chinese Medicine, Shanghai 201203, China

³ Nanjing Institute of Geology and Palaeontology, Chinese Academy of Sciences, Nanjing 210008, China

⁴ Shanghai Key Laboratory of Plant Functional Genomics and Resources, Shanghai Chenshan Botanical Garden, Shanghai 201602, China

* Corresponding authors, E-mail: xiaoyingtc@shutcm.edu.cn; xuejingshi@shnu.edu.cn

Abstract

Sporopollenin, a key adaptation enabling plants' transition to terrestrial environments, shields spores and pollen from UV damage, ensuring their survival and dispersal on land. The concentration of UV-absorbing *p*-CA and ferulic acids within sporopollenin correlates with UV levels, offering a proxy for reconstructing UV irradiance. However, the composition of UV-absorbing compounds varies across species, and a universal marker linking sporopollenin chemistry to UV resistance has yet to be identified. Given that UV-absorbing components may convert UV radiation into visible light, we developed a method to quantify the Integral of Sporopollenin Autofluorescence Intensity (ISAI), a novel parameter hypothesized to reflect pollen UV resistance. We analyzed ISAI in spores/pollen from 55 plant species and 18 *Arabidopsis thaliana* ecotypes. Our results reveal significant ISAI variation, which associates with solar-irradiance gradients. Species exposed to sunlight exhibited higher ISAI values than those adapted to shaded environments. Plants flowering during periods of elevated solar radiation displayed increased ISAI. Notably, analysis of *A. thaliana* ecotypes demonstrated that ISAI is heritable and correlated with pollen UV resistance. This study indicates ISAI as a metric in spore and pollen research, linking sporopollenin autofluorescence to UV adaptation. ISAI provides a novel tool for investigating plant responses to UV environments.

Citation: Jia XL, Wang XL, Chen YY, Mao LM, Shen H, et al. 2025. Integral of Sporopollenin Autofluorescence Intensity (ISAI), a novel marker for UV adaptation in spores/pollen. *Seed Biology* 4: e017 <https://doi.org/10.48130/seedbio-0025-0016>

Introduction

Land plants are sessile organisms with life cycles alternating between diploid sporophyte and haploid gametophyte generations. This alternation is mediated by meiosis, which produces spores or their derived homologs, pollen. Bryophytes, lycophytes, and ferns are spore-producing plants that rely on spores for dispersal^[1]. In seed plants, pollen delivers male gametes to the stigma, enabling sexual reproduction^[2,3]. During dispersal, spores and pollen of land plants are directly exposed to atmospheric stressors like desiccation and ultraviolet (UV) radiation without the protection of water. To ensure survival and reproductive success, plants have evolved strategies to protect spores/pollen from environmental stresses^[4]. Among these stressors, ultraviolet B (UV-B) radiation (290–320 nm) poses a significant threat by inducing DNA damage^[5]. Land plants primarily mitigate UV-B damage through UV-B absorption and DNA repair mechanisms^[5,6]. However, spores and pollen, as metabolically inactive haploid gametophytes with dehydrated DNA, are exceptionally sensitive to UV-B^[7]. Exposure to UV-B often reduces pollen quantity and causes structural malformations^[8–10], underscoring the critical role of UV-B absorption in protecting these reproductive units.

Spores/pollen are covered by an outer cell wall exine, which is mainly constituted by sporopollenin^[11]. The sporopollenin is the major structure for absorbing UV radiation^[12–14]. Recent studies show that both phenylpropanoid phenolics and naringenin are components of sporopollenin^[15–19]. Chemical evidence indicates that the phenolics are linked by C-C bonds to form the core structure of

the sporopollenin, and naringenin may be linked to the core structure by ester bonds^[20]. Genetic evidence shows that the phenolics and naringenin in sporopollenin are involved in the UV defense of pollen in *Arabidopsis*^[15–17]. Moreover, the abundance of *para*-coumaric acid (*p*-CA) and ferulic acid (FA) in sporopollenin correlates with ambient UV-B levels, enabling their use as proxies for reconstructing historical UV irradiance^[12,21–27]. However, Nuclear Magnetic Resonance Spectroscopy (NMR) analysis indicates that besides *para*-coumaric acid and ferulic acid, *para*-hydroxybenzoate, naringenin, lignin guaiacyl (G) unit, and cinnamyl alcohol groups are also present in the sporopollenin, which may also have the ability to absorb UV-B^[15,16,20]. Furthermore, different plants accumulate distinct phenolics in their sporopollenin^[15]. Identifying a universal sporopollenin-based marker for UV resistance could advance studies of plant reproductive evolution.

Sporopollenin autofluorescence is widely observed in land plants^[13,15,28,29]. In this study, we established a method to quantify the Integral of Sporopollenin Autofluorescence Intensity (ISAI), which is a potential parameter for indicating the pollen UV resistance ability. The ISAI was analyzed in 55 representative land plants. We showed that the ISAI variations in spores/pollen are associated with the solar irradiance gradients. Using 18 *Arabidopsis* ecotypes, we further demonstrate that ISAI is heritable and correlates with pollen UV resistance. Our findings establish ISAI as a diagnostic parameter for assessing spores/pollen UV tolerance, offering insights into plant adaptation to terrestrial environments.

Materials and methods

Plant materials and growth conditions

Spores of *Marchantia polymorpha*, *Haplocladium microphyllum*, *Funaria hygrometrica*, *Palhinhaea cernua*, *Phlegmariurus phlegmaria*, *Isoetes sinensis*, *Ophioglossum vulgatum*, *Lygodium japonicum*, and *Pteris multifida*, pollen of *Cycas revoluta*, *Cedrus deodara*, *Cryptomeria japonica*, *Metasequoia glyptostroboides*, *Nymphaea tetragona*, *Nelumbo nucifera*, *Yulania denudata*, *Typha orientalis*, *Iris pseudacorus*, *Crocasmia × crocosmiiflora*, *Ophiopogon bodinieri*, *Hosta plantaginea*, *Trachycarpus fortunei*, *Nandina domestica*, *Juglans regia*, *Salix babylonica*, *Calystegia hederacea*, *Petunia × hybrida*, *Vitex negundo*, *Salvia japonica*, *Thymus mongolicus*, *Nerium oleander*, *Lantana camara*, *Mimulus hybridus*, *Paulownia fortunei*, *Veronica arvensis*, *Ligustrum lucidum*, *Osmanthus fragrans*, *Fraxinus chinensis*, *Chrysosaminum floridum*, *Cirsium japonicum*, *Helianthus tuberosus*, *Cnidium monnieri*, *Cuphea hyssopifolia*, *Lythrum salicaria*, *Punica granatum*, *Oxalis corniculata*, *Malus halliana*, *Prunus × yedoensis*, *Spiraea thunbergii*, *Rosa multiflora*, *Cercis chinensis*, *Trifolium repens*, *Wisteria sinensis*, *Sedum lineare*, and *Orychophragmus violaceus* were collected in Shanghai, China. All the spores/pollen used in this study were collected from plants grown outdoors under natural light conditions. For each species, spores or pollen were sampled from multiple plants and loaded into a 1.5 mL EP tube. All the samples were stored at -80°C until use. The *A. thaliana* Columbia-0 (Col-0) was preserved in our lab. The ecotype seeds used in this study, CS76412 (Fei-0), CS76449 (Bik-1), CS76468 (Co-1), CS76485 (Est), CS76526 (Kil-0), CS76558 (Na-1), CS76572 (Pi-0), CS76598 (Seattle-0), CS76623 (Van-0), CS76626 (Wa-1), CS76883 (Gol-2), CS77013 (LDV-18), CS77040 (LIN S-5), CS77389 (Tsu-0), CS78787 (Set-1), CS78791 (UKID96), and CS78853 (WAR) were obtained from the Arabidopsis Biological Resource Center (ABRC) (<https://abrc.osu.edu>)^[30]. All these ecotypes of *A. thaliana* were grown under long-day conditions (16 h light/8 h dark) in a $\sim 22^{\circ}\text{C}$ plant incubator, light intensity of 8,000 lux. After three generations were used for this study. Pollen grains from four independent plants were collected and loaded into a 1.5 mL EP tube. All the samples were stored at -80°C until use.

Pollen germination assays and UV-B treatment

The pollen germination assay was performed as described previously^[15]. Briefly, fine-tipped tweezers were used to smear the pollen from four plants per ecotype evenly on two round dishes covered with germination medium (sucrose 18%, H_3BO_3 0.01%, CaCl_2 1 mM, $\text{Ca}(\text{NO}_3)_2$ 1 mM, MgSO_4 1 mM, Low melting Agarose 1.5%, pH ~ 7.0) through the binocular stereo anatomy microscope (SHL-7045, Shenzhen Shunhuali Electronics Co, China). One dish from each pair received UV-B treatment (the UV-B treatment energy was set to simulate the UV-B intensity encountered during summer noon in southern China: 302 nm peak wavelength, 1.2 W/cm^2 irradiance, 7.5 min exposure) using a UV crosslinker (UV-100, Tanon Science & Technology Co., China). Both treated and untreated pollen were incubated at 24°C for 16 h in the dark. Germination rates were quantified using an Olympus BX51 microscope (Olympus Corp., Japan) with integrated digital imaging. For statistical analysis, ≥ 200 pollen grains per replicate were analyzed using ImageJ. Four biological replicates (independent plants) were assessed.

Scanning electron microscopy (SEM)

Spores/pollen were mounted on SEM stubs, and the mounted samples were then coated with palladium-gold in a sputter coater (pattern) and examined via SEM (SU-8010; HITACHI, www.hitachi.com.cn) with an acceleration voltage of 2.0 kV.

Confocal microscopy

The LSCM fluorescence images were obtained with a Leica STELLARIS 8 laser scanning confocal microscopy (LSCM) (STELLARIS 8, Leica Co, Germany). Spores/pollen were mounted using 1% low-melting-point agarose solution as the mounting medium. To monitor spore/pollen wall autofluorescence, a 405 nm laser line was used for excitation, and emission spectra were recorded in the range of 450–550 nm. The 63 \times plan apochromats objective (#506350, Leica Co, Germany) was used. For sporopollenin wall autofluorescence of *A. thaliana* ecotypes, the smart intensity was set as 1.0%, the smart gain was set as 120.0%, and the pinhole was set as 1.00 AU. For sporopollenin wall autofluorescence of other tested species, the smart intensity was set as 0.4%, the smart gain was set as 60.0%, and the pinhole was set as 1.00 AU. LAS X (LAS_X_3.3.0_16799, Leica Co, Germany) software was used for the data analysis.

Computing method of the integral autofluorescence of the spore/pollen wall

The auto-fluorescence images at the maximum light section of pollen in the equatorial view were obtained by using the LSCM. The signal intensity of the spore/pollen wall along the distal-proximal axial was extracted by using the line profile, which was provided by LAS X (Leica Co, Germany) software. Using the software of OriginPro 2021 (OriginPro Learning Edition, www.originlab.com), the line chart was created, and the auto-fluorescence of the spore/pollen wall was estimated from the integral area. Twelve sites of each spore/pollen were selected for line profiling. For spores/pollen collected from outdoors, nine spores or pollen grains of each species were analyzed, while for *Arabidopsis* cultivated in a plant incubator, five pollen grains of each *Arabidopsis* ecotype were measured.

Measurement of pollen size and pollen wall thickness

Pollen grains from *A. thaliana* ecotypes were imaged by SEM. The Polar axis of the pollen was defined as the pollen size. Forty pollen grains were selected from each ecotype, and the pollen size was measured by ImageJ. To measure the pollen wall thickness, pollen from *A. thaliana* ecotypes and other land plants were dusted into glass vials and mounted on glass microscope slides^[31], imaging at the maximum light section of pollen. The pollen wall thickness was measured by ImageJ. Ten sites of each pollen and nine independent pollen grains were selected for measurement of the pollen wall thickness in all these plants.

Data handling

To analyze what determines the pollen UV-B resistance ability, we calculated the decline rate of pollen germination of *A. thaliana* ecotypes tested. And the pollen characteristics, including the pollen wall thickness, the pollen size, and the integral of sporopollenin wall autofluorescence, were measured with the software of ImageJ and OriginPro 2021, respectively. For correlation analysis, we used Spearman correlation analysis to evaluate the effect of pollen characteristics on the UV-B defenses ability in different *A. thaliana* ecotypes. To analyze the variation of pollen wall thickness, pollen size, and integral of sporopollenin wall autofluorescence into group and inter-group, we used GraphPad Prism 8.0 (GraphPad Software, www.graphpad.com) for one-way ANOVA and Tukey's Method for multiple comparisons. The family-wise alpha threshold and confidence level were set as 0.05 (95% confidence interval). To compare the difference of autofluorescence intensity in pollen wall between different plant groups, OriginPro 2021 was used for Mann-Whitney *U* test. The confidence level was set as 0.05 (95% confidence interval). The data of monthly solar irradiation of East China was plotted with GraphPad Prism 8.0 and fitted with Smoothing spline.

Results

Quantification of ISAI by using laser scanning confocal microscopy (LSCM)

During pollen dispersal, harmful UV radiation must penetrate the pollen wall to reach the cytoplasm, where it can cause damage (Fig. 1a). Under UV irradiation, the pollen wall exhibits autofluorescence, with a maximum emission wavelength at 450–550 nm^[15,29]. The autofluorescence intensity of the pollen wall may reflect its capacity to convert short-wave UV radiation into less harmful long-wave visible light. Consequently, mapping the autofluorescence intensity along the distal-proximal axis of the pollen wall could serve as a functional indicator of UV resistance (Fig. 1a). Autofluorescence images were acquired at the equatorial maximum optical section of pollen grains using LSCM (Supplementary Fig. S1). Signal intensity along the distal-proximal axis of the pollen wall was extracted, defining a parameter termed the 'Integral of Sporopollenin Autofluorescence Intensity (ISAI)' (Fig. 1b).

ISAI variations in spores/pollen are associated with the solar irradiance gradients

Land plants, including bryophytes, pteridophytes, and seed plants, occupy distinct ecological niches, leading to differential exposure to UV radiation within the same geographical region. To investigate this relationship, spores and pollen were collected from common land plants in the Shanghai area, East China, and analyzed for ISAI (Fig. 2a; Supplementary Figs S2 & S3, Supplementary Tables

S1 & S2). In this area, seed plant pollen is typically exposed to direct sunlight, while pteridophyte spores occupy shaded understory layers with reduced UV exposure. Bryophytes, often growing in damp, shaded microhabitats, experience the lowest UV radiation. Consistent with these ecological differences, the highest ISAI was observed in seed plants (Fig. 2b). Statistical analysis using the Mann-Whitney *U* test revealed significant differences in ISAI between bryophytes and pteridophytes, as well as between pteridophytes and seed plants (Fig. 2c). These results indicate that solar irradiance gradients influence ISAI levels in pollen and spores.

Notably, while many seed plant species exhibited high ISAI, others displayed values comparable to pteridophytes (Fig. 2). Seed plants produce pollen across different seasons, during which solar UV radiation varies significantly^[32]. East China's subtropical monsoon climate features intense UV radiation from June to August (Fig. 3a). The relationship between seasonal UV radiation and ISAI was analyzed. Plants with higher pollen ISAI predominantly flowered during high-radiation seasons (Fig. 3b). Based on monthly average radiation levels in East China, species flowering between June and August were classified as high-solar-radiation groups, while others were categorized as low-solar-radiation groups (Supplementary Table S3). Plants flowering under high solar radiation exhibited significantly higher ISAI than those in low-radiation periods (Fig. 3c). Furthermore, all species with extreme ISAI values belonged to the high-radiation group (Fig. 3c), consistently supporting the hypothesis that ISAI elevation is associated with high UV radiation environments.

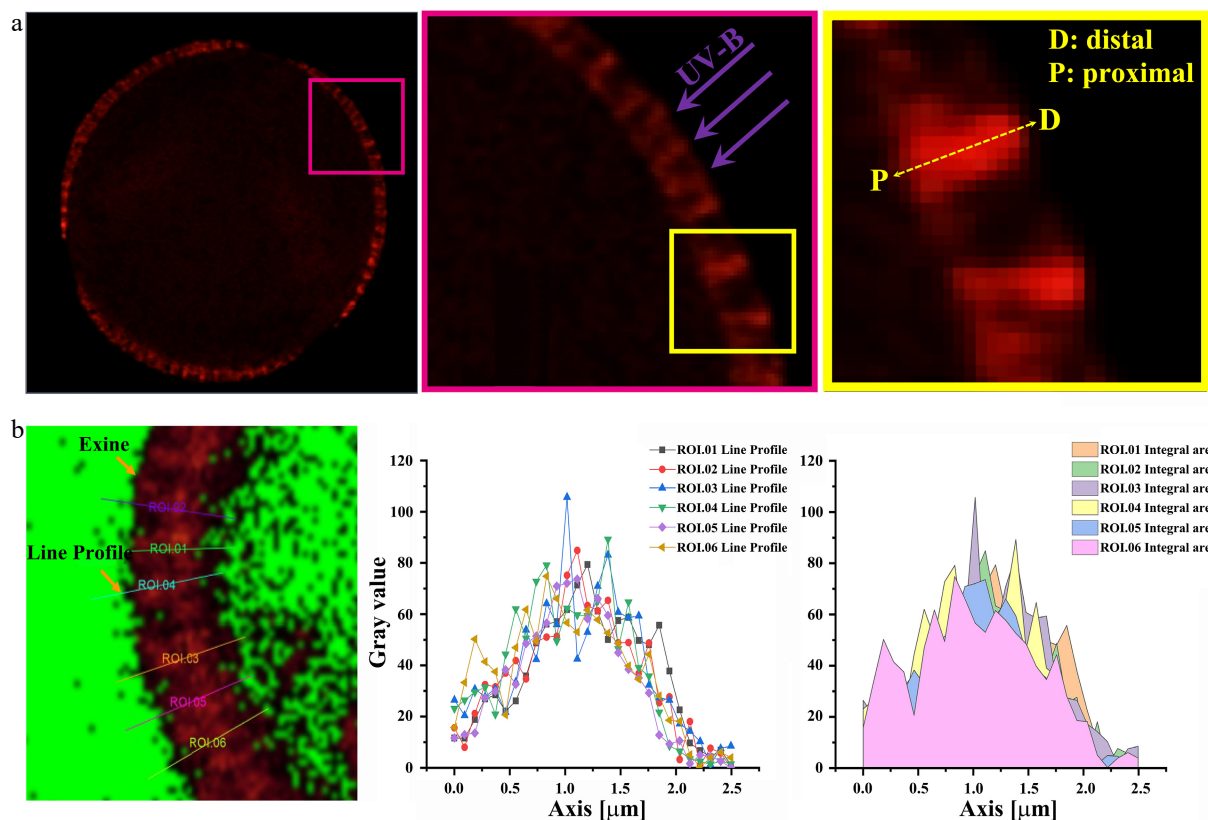


Fig. 1 The quantification of ISAI by using laser scanning confocal microscopy (LSCM). (a) The LSCM image of the maximum light section of spore/pollen wall in equatorial view. Left: the maximum light section of the spore/pollen in equatorial view. Middle: the magnified image of the pink box in the left image. UV-B damage the protoplasm only after they pass through the pollen wall. Right: the diagrammatic sketch of the distal-proximal axial of spore/pollen wall, and it is the magnified image of the yellow box in the middle image. UV-B damage the protoplasm only after they pass through the pollen wall along the distal-proximal axial. (D: distal; P: proximal). (b) Detection of autofluorescent intensity of the pollen by LSCM. ROI: region of interest. Left image: the diagram of the line profile of the pollen wall autofluorescence. The image is in the maximum light section of spore/pollen in the equatorial view. The signal intensity of exine was obtained using the line profile provided by LAS X (Leica) software. Middle image: line chart of the autofluorescent intensity of the pollen wall. Right image: the signal intensity of the pollen wall autofluorescent was obtained by using the method of integral area.

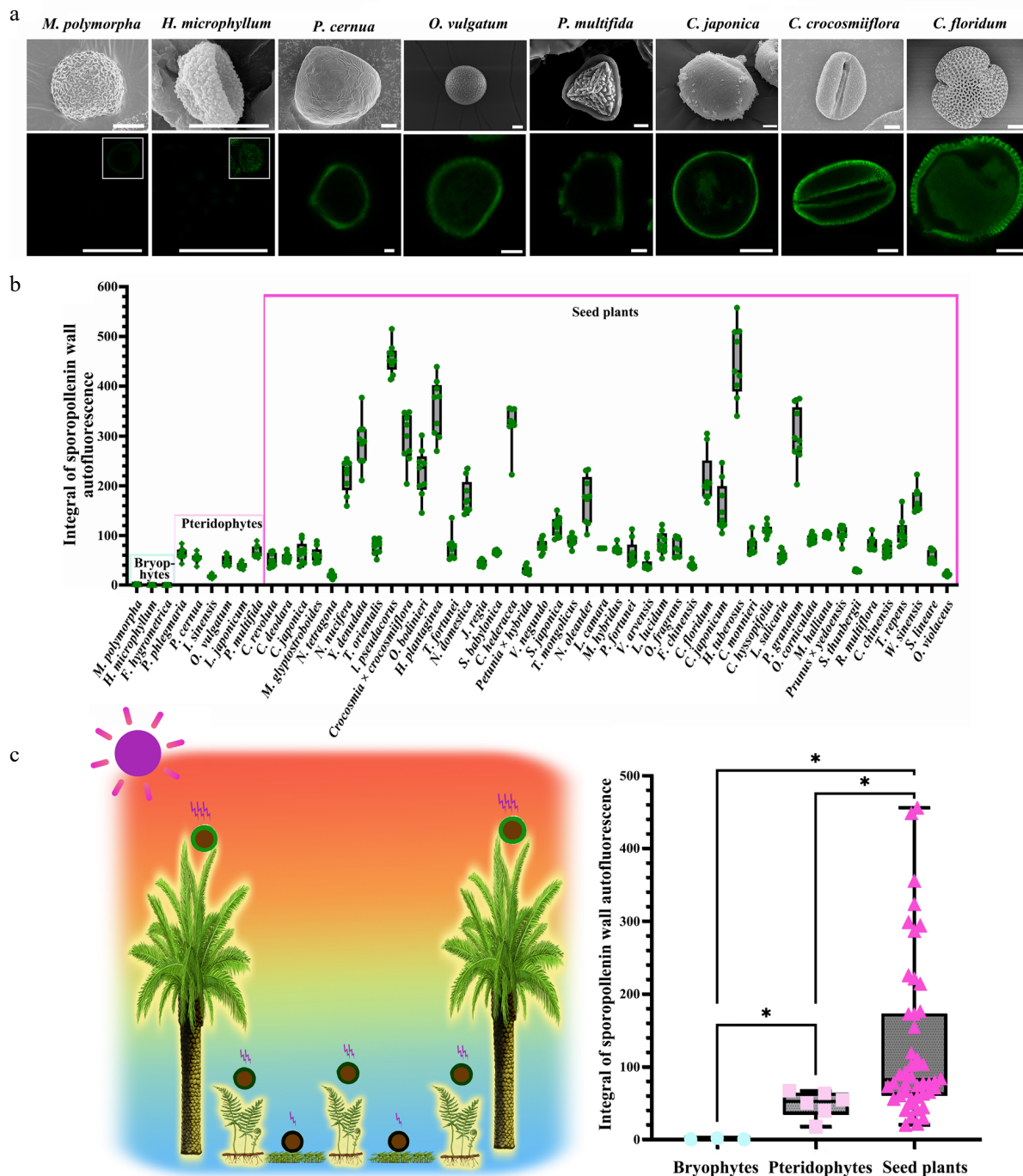


Fig. 2 ISAI varies among spores/pollen from distinct ecological niches. (a) Scanning electron microscope (SEM) and auto-fluorescence (Auto-flu) images of spore/pollen of several representative species. For SEM, scale bars = 10 μm ; for LCSM, scale bars = 10 μm . For *M. polymorpha* and *H. microphyllum*, since the sporopollenin wall autofluorescence is very low, the picture with the image dynamic range adjusted is displayed in the upper right corner of the fluorescence picture. (b) Columnar diagram of spore/pollen wall autofluorescent intensity, 12 sites of each spore/pollen were selected for line profile, and nine spores or pollen grains were counted from each species. (mean \pm SD, $n = 9$). (c) Statistical analysis of spore/pollen wall autofluorescent intensity. Left: summary of UV-B irradiation experienced by spores/pollen of land plants. Due to variations in the ecological niches of land plants and the spread distance of spores/pollen, the UV-B radiation experienced by spores/pollen in the terrestrial environment differ. Specifically, UV radiation intensities typically follow the order of seed plants > pteridophytes > bryophytes. Right: autofluorescent intensity of spore/pollen wall showed significant differences among bryophytes, pteridophytes, and seed plants (Mann-Whitney U test: Bryophytes vs Pteridophytes: $Z = -2.19469$, $p = 1.19\text{E-}2$; Bryophytes vs Seed plants: $Z = -2.85665$, $p = 5.43\text{E-}5$; Pteridophytes vs Seed plants: $Z = -2.62071$, $p = 3.14\text{E-}3$; *, $p < 0.05$).

Heritable ISAI of *Arabidopsis* ecotypes is correlated with pollen UV resistance

Previous studies indicate that plants accumulate higher levels of UV-absorbing compounds in the pollen wall when briefly exposed to UV radiation during development^[12]. To investigate whether ISAI

variation arises solely from solar UV exposure during spores/pollen development or is partly attributable to heritable genetic variation, and the association between ISAI and the UV resistance capacity of pollen, we analyzed multiple *Arabidopsis thaliana* ecotypes. *Arabidopsis thaliana*, a globally distributed species, has evolved

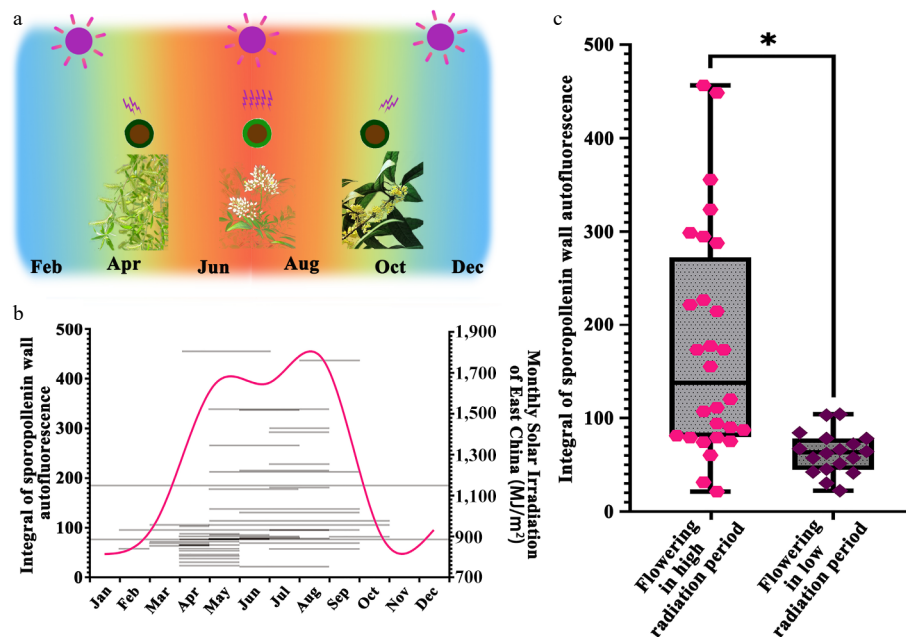


Fig. 3 Pollen ISAI of seed plants across different flowering periods. (a) Summary of UV-B irradiation experienced by the pollen of land plants in East China. East China's subtropical monsoon climate features intense UV radiation from June to August, during which flowering species may subject their pollen to increased solar irradiation. (b) Summary of florescence, integral of sporopollenin wall autofluorescence intensity, and the monthly solar irradiation of East China. The grey lines show the florescence and the integral of sporopollenin wall autofluorescence intensity of seed plants tested. The magenta line shows the variation of monthly solar irradiation of East China. The tested seed plants have different florescence and integral of sporopollenin wall autofluorescence intensity. (c) Statistical analysis of autofluorescent intensity of pollen wall of seed plants which flower under high and low radiation conditions. The pollen wall autofluorescence is significantly different between species which flowering in high radiation environment and low radiation environment (Mann-Whitney U test: Flowering in high radiation period vs Flowering in low radiation period: $Z = -4.10761$, $p = 1.23E-5$; *, $p < 0.05$).

distinct ecotypes adapted to diverse environments^[33,34]. This makes it an excellent research object for bridging field studies and laboratory studies. In this study, 81 ecotypes sourced from varied environments were obtained from the Arabidopsis Biological Resource Center (ABRC). Under long-day conditions (16 h light/8 h dark, ~22 °C growth chamber, 8,000 lux light intensity), 41 ecotypes failed to flower. Of the remaining, 22 exhibited varying degrees of delayed flowering. Eighteen ecotypes with comparable growth rates were selected for the study, including four from North America's eastern and western coasts, 11 from across Europe, two from East and West Asia, and Col-0 (Fig. 4a). These ecotypes were grown in a plant incubator for three generations to minimize effects of prior environmental disparities. Pollen ISAI analysis revealed significant variation among ecotypes (Fig. 4b; Supplementary Table S4), demonstrating that genetic variation contributes to ISAI differences.

Furthermore, pollen germination rates of these ecotypes under UV-B treatment were evaluated (302 nm, 7.5 min, 1.2 W/cm²) (Supplementary Fig. S4). Germination rates were normalized to untreated controls (set as 100%), with post-treatment reductions defined as 'pollen germination decline rates'. Ecotypes exhibited divergent decline rates (Fig. 4c, Supplementary Table S5). Spearman's rank correlation analysis revealed a significant negative association between ISAI and pollen germination decline ($\rho = -0.60$, $p = 0.009$) (Fig. 4d), indicating that higher ISAI correlates with stronger UV-B resistance. In addition, we showed that pollen size varied significantly among ecotypes, whereas pollen wall thickness showed no significant differences (Supplementary Figs S5 & S6, Supplementary Tables S6 & S7), and the ISAI had no correlation with the pollen wall thickness ($\rho = 0.35$, $p = 0.160$) (Supplementary Fig. S7), suggesting ISAI is influenced by pollen wall chemistry rather than thickness. These results demonstrate natural variation in sporopollenin chemistry, with ISAI, a chemically determined trait, positively linked to pollen UV-B resistance.

Genetic evidence demonstrates that phenylpropanoid phenolics are essential for ISAI

Recent studies identified *para*-coumaric acid, ferulic acid, *para*-hydroxybenzoate, naringenin, lignin G units, and cinnamyl alcohol as sporopollenin components^[20]. In *Arabidopsis*, these compounds are synthesized via the phenylpropanoid pathway^[35]. Within this pathway, CINNAMATE-4-HYDROXYLASE (C4H) catalyzes the conversion of cinnamic acid to *para*-coumaric acid. This intermediate is subsequently metabolized: CINAMOYL-CoA REDUCTASE (CCR) converts it into hydroxycinnamyl alcohols and ultimately into lignin units, while Chalcone Synthase (CHS) channels it into flavonoids^[36–38]. To investigate the function of phenylpropanoid pathway in ISAI, we collected pollen from Col-0, *ref3-1* (mutant of C4H gene), *ccr1-4* (mutant of CCR gene), and *chs* (mutant of CHS gene). ISAI was dramatically reduced in both *ref3-1* and *ccr1-4* mutants (Supplementary Fig. S8), indicating that *para*-coumaric acid and its downstream products hydroxycinnamyl alcohols and lignin units are essential for pollen ISAI. Both flavonoid and hydroxycinnamyl alcohol/lignin biosynthesis share *para*-coumaric acid as a common precursor. Blocking flavonoid synthesis in the *chs* mutant likely redirects this precursor flux towards hydroxycinnamyl alcohol/lignin production. Consistent with this metabolic shift, we observed increased ISAI in the *chs* mutant (Supplementary Fig. S8). Taken together, these results demonstrate that phenylpropanoid-derived phenolics are essential for ISAI.

Discussion

ISAI serves as a key parameter in pollen/spore studies, demonstrating significant correlation with UV resistance

In this study, we developed a method to measure the intensity of sporopollenin wall autofluorescence by using LSM (Fig. 1). We

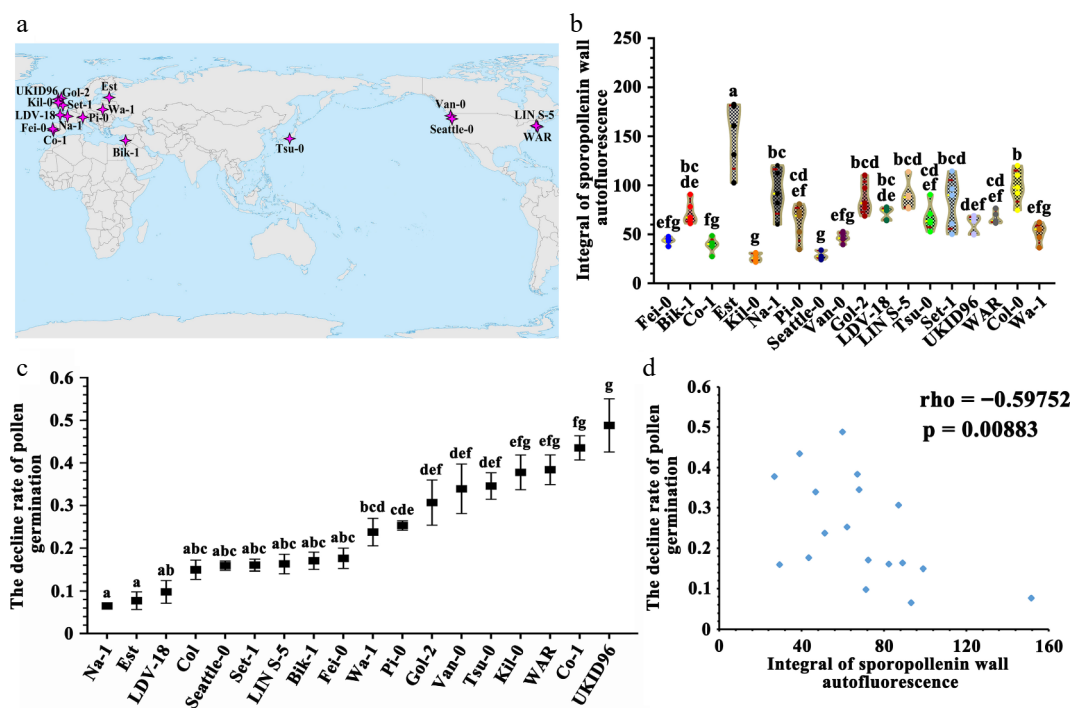


Fig. 4 The sporopollenin wall autofluorescence is correlated with UV-B defense ability of pollen grains in *Arabidopsis thaliana* ecotypes. (a) The geographical distribution of ecotypes used in this experiment. (b) Violin plot of the integral of sporopollenin wall autofluorescence intensity in *A. thaliana* ecotypes. The yellow line indicates the average value, the red line indicates the quartile value, and the data points are showed in the graph. Twelve measurement lines each pollen grain, five pollen grains each *A. thaliana* ecotype (mean \pm SD, $n = 5$). Grouping information using the Tukey's Method and 95% confidence. Means that do not share a letter are significantly different. The *A. thaliana* ecotypes showed significant difference in the integral of sporopollenin wall autofluorescence. (c) Determination of pollen germination rate (mean \pm SD, $n = 4$). Grouping information using Tukey's method and 95% confidence. Means that do not share a letter are significantly different. These *A. thaliana* ecotypes showed different decline rates under the UV-B treatment. (d) Spearman correlation analysis of the decline rates of pollen germination under the UV-B treatment in different *A. thaliana* ecotypes vs the integral of sporopollenin wall autofluorescence intensity (Spearman correlation: $\rho = -0.59752$, $p = 0.00883$).

analyzed the ISAI of 55 representative land plants collected from the wild and 18 *Arabidopsis* ecotypes cultivated in the laboratory (Figs 2, 4; Supplementary Figs S2, S3). The results show that the ISAI is associated with the intensity of environmental radiation encountered by spores/pollen. All seed plants with high ISAI values flower during summer months (Fig. 3); seed plants flowering in low-radiation seasons showed comparable ISAI levels to pteridophytes (Supplementary Fig. S9); and *Arabidopsis* ecotypes exhibited pollen UV resistance capacities that are correlated to their ISAI values. These findings collectively indicate ISAI enhancement as an adaptive response to high-radiation environments. The results align with prior chemical studies showing UV-B-dependent phenolic acid variations in sporopollenin^[12,22–24,39], while introducing LSCM-based ISAI analysis as a novel nondestructive method requiring minimal samples. Methodological advantages encompass the absence of complex pretreatment and the capability to acquire quantitative data directly reflecting the pollen UV resistance ability from individual pollen grains *in-situ*, which expands current UV-B reconstruction methods.

Natural selection may act on genes regulating spore/pollen wall components, thereby increasing the ISAI and UV-B resistance

Organismal adaptation to environmental change involves both short-term plastic responses and long-term genetic modifications^[40–42]. Understanding these adaptive mechanisms, particularly under shifting environmental pressures, remains a central focus in evolutionary biology. Prior studies have explored short-term environmental stressors, such as altered radiation levels, on pollen autofluorescence^[21,31,43–46]. In this study, we analyzed

Arabidopsis ecotypes collected from diverse ecological habitats. As shown in Fig. 4, ecotypes that grow under identical conditions exhibit distinct ISAI levels, which correlate with their UV-B resistance. Further analysis reveals no significant correlation between pollen size or wall thickness and either ISAI or UV adaptation (Supplementary Figs S5–S7, S10, S11). This suggests that genetic variation primarily shapes pollen wall composition (rather than pollen wall thickness), which is critical for ISAI in *Arabidopsis*. Furthermore, analysis across land plants also demonstrates that ISAI is not correlated with pollen or spore wall thickness (Supplementary Fig. S12, Supplementary Tables S8, S9). Supporting this, fluorescent analysis indicates divergent sporopollenin compositions among different land plants^[15], highlighting the critical role of sporopollenin chemistry in pollen UV adaptation. ISAI arises primarily from autofluorescent compounds. Genetic evidence shows that mutants defective in the phenylpropanoid pathway have reduced ISAI and decreased UV-defense ability, underscoring the pathway's critical role^[15]. These findings imply that genes in regulating the phenylpropanoid pathway are likely the targets of natural selection to enhance UV-B defense in spores and pollen. Future studies into the mechanisms underlying of this selection process, as well as the relative contributions of short-term plasticity and long-term genetic alterations in species' environmental adaptation, will deepen our comprehension of spores/pollen to the changing UV radiation.

Author contributions

The authors confirm their contributions to the paper as follows: experiments conception and design: Xue JS, Xiao Y, Yang ZN, Jia XL; experiments performing: Xue JS, Jia XL, Chen YY, Wang XL, Mao LM;

data analysis: Xue JS, Jia XL, Mao LM, Yang ZN; manuscript writing: Xue JS, Yang ZN, Jia XL, Mao LM, Shen H. All authors reviewed the results and approved the final version of the manuscript.

Data availability

All data generated or analyzed during this study are included in this published article and its supplementary information files, further inquiries are available from the corresponding author upon reasonable request.

Acknowledgments

This work was supported by grants from the National Natural Science Foundation of China (31900165), Shanghai Municipal Education Commission (2019-01-07-00-02-E00006), Science and Technology Commission of Shanghai Municipality (17DZ2252700, 18DZ2260500, and 21DZ2202300), and the Postdoctoral Fellowship Program (Grade C) of China Postdoctoral Science Foundation (GZC20231699). We would like to thank Dr. Zong-Xin Ren (Kunming Institute of Botany, Chinese Academy of Sciences) for the helpful comments on the manuscript.

Conflict of interest

The authors declare that they have no conflict of interest.

Supplementary information accompanies this paper at (<https://www.maxapress.com/article/doi/10.48130/seedbio-0025-0016>)

Dates

Received 14 April 2025; Revised 28 July 2025; Accepted 11 August 2025; Published online 10 October 2025

References

- Jill Harrison C. 2017. Development and genetics in the evolution of land plant body plans. *Philosophical Transactions of the Royal Society B, Biological Sciences* 372:20150490
- Wallace S, Fleming A, Wellman CH, Beerling DJ. 2011. Evolutionary development of the plant and spore wall. *AoB Plants* 2011:plr027
- Bai SN. 2017. Reconsideration of plant morphological traits: from a structure-based perspective to a function-based evolutionary perspective. *Frontiers in Plant Science* 8:345
- Ariizumi T, Toriyama K. 2011. Genetic regulation of sporopollenin synthesis and pollen exine development. *Annual Review of Plant Biology* 62:437–60
- Shi C, Liu H. 2021. How plants protect themselves from ultraviolet-B radiation stress. *Plant Physiology* 187:1096–103
- Chen Z, Dong Y, Huang X. 2022. Plant responses to UV-B radiation: signaling, acclimation and stress tolerance. *Stress Biology* 2:51
- Musil CF. 1995. Differential effects of elevated ultraviolet-B radiation on the photochemical and reproductive performances of dicotyledonous and monocotyledonous arid-environment ephemerals. *Plant, Cell & Environment* 18:844–54
- Benca JP, Duijnste IAP, Looy CV. 2018. UV-B-induced forest sterility: implications of ozone shield failure in Earth's largest extinction. *Science Advances* 4:e1700618
- Gray LA, Varga S, Soulsbury CD. 2024. Increased UV intensity reduces pollen viability in *Brassica rapa*. *Flora* 319:152582
- Cun S, Zhang C, Chen J, Qian L, Sun H, et al. 2024. Effects of UV-B radiation on pollen germination and tube growth: a global meta-analysis. *Science of The Total Environment* 915:170097
- Grienenberger E, Quilichini TD. 2021. The toughest material in the plant kingdom: an update on sporopollenin. *Frontiers in Plant Science* 12:703864
- Rozema J, Broekman RA, Blokker P, Meijkamp BB, de Bakker N, et al. 2001. UV-B absorbance and UV-B absorbing compounds (*para*-coumaric acid) in pollen and sporopollenin: the perspective to track historic UV-B levels. *Journal of Photochemistry and Photobiology B: Biology* 62:108–17
- Willemse MTM. 1972. Changes in the autofluorescence of the pollen wall during microsporogenesis and chemical treatments. *Acta Botanica Neerlandica* 21:1–16
- Dobritsa AA, Geanconteri A, Shrestha J, Carlson A, Kooyers N, et al. 2011. A large-scale genetic screen in *Arabidopsis* to identify genes involved in pollen exine production. *Plant Physiology* 157:947–70
- Xue JS, Zhang B, Zhan H, Lv YL, Jia XL, et al. 2020. Phenylpropanoid derivatives are essential components of sporopollenin in vascular plants. *Molecular Plant* 13:1644–53
- Xue JS, Qiu S, Jia XL, Shen SY, Shen CW, et al. 2023. Stepwise changes in flavonoids in spores/pollen contributed to terrestrial adaptation of plants. *Plant Physiology* 193:627–42
- Hsieh K, Huang AHC. 2007. Tapetosomes in *Brassica tapetum* accumulate endoplasmic reticulum-derived flavonoids and alkanes for delivery to the pollen surface. *The Plant Cell* 19:582–96
- Nierop KGJ, Versteegh GJM, Filley TR, de Leeuw JW. 2019. Quantitative analysis of diverse sporomorph-derived sporopollenins. *Phytochemistry* 162:207–15
- Quilichini TD, Grienenberger E, Douglas CJ. 2015. The biosynthesis, composition and assembly of the outer pollen wall: a tough case to crack. *Phytochemistry* 113:170–82
- Chen X, Huang DD, Xue JS, Bu JH, Guo MQ, et al. 2024. Polymeric phenylpropanoid derivatives crosslinked by hydroxyl fatty acids form the core structure of rape sporopollenin. *Nature Plants* 10:1790–800
- Rozema J, Noordijk AJ, Broekman RA, van Beem A, Meijkamp BM, et al. 2001. (Poly)phenolic compounds in pollen and spores of Antarctic plants as indicators of solar UV-B—a new proxy for the reconstruction of past solar UV-B? *Plant Ecology* 154:9–26
- Blokker P, Yeloff D, Boelen P, Broekman RA, Rozema J. 2005. Development of a proxy for past surface UV-B irradiation: a thermally assisted hydrolysis and methylation py-GC/MS method for the analysis of pollen and spores. *Analytical Chemistry* 77:6026–31
- Willis KJ, Feurdean A, Birks HJB, Bjune AE, Breman E, et al. 2011. Quantification of UV-B flux through time using UV-B-absorbing compounds contained in fossil *Pinus* sporopollenin. *New Phytologist* 192:553–60
- Jardine PE, Fraser WT, Lomax BH, Sephton MA, Shanahan TM, et al. 2016. Pollen and spores as biological recorders of past ultraviolet irradiance. *Scientific Reports* 6:39269
- Bell BA, Fletcher WJ, Ryan P, Seddon AWR, Wogelius RA, et al. 2018. UV-B-absorbing compounds in modern *Cedrus atlantica* pollen: the potential for a summer UV-B proxy for Northwest Africa. *The Holocene* 28:1382–94
- Seddon AWR, Festi D, Robson TM, Zimmermann B. 2019. Fossil pollen and spores as a tool for reconstructing ancient solar-ultraviolet irradiance received by plants: an assessment of prospects and challenges using proxy-system modelling. *Photochemical & Photobiological Sciences* 18:275–94
- Liu F, Peng H, Marshall JEA, Lomax BH, Bomfleur B, et al. 2023. Dying in the Sun: direct evidence for elevated UV-B radiation at the end-Permian mass extinction. *Science Advances* 9:eabo6102
- Mitsumoto K, Yabusaki K, Aoyagi H. 2009. Classification of pollen species using autofluorescence image analysis. *Journal of Bioscience and Bioengineering* 107:90–94
- O'Connor DJ, Iacopino D, Healy DA, O'Sullivan D, Sodeau JR. 2011. The intrinsic fluorescence spectra of selected pollen and fungal spores. *Atmospheric Environment* 45:6451–58
- The 1001 Genomes Consortium. 2016. 1, 135 Genomes reveal the global pattern of polymorphism in *Arabidopsis thaliana*. *Cell* 166:481–91
- Yeloff D, Blokker P, Boelen P, Rozema J. 2008. Is pollen morphology of *Salix polaris* affected by enhanced UV-B irradiation? Results from a field experiment in high Arctic tundra. *Arctic, Antarctic & Alpine Research* 40:770–74

32. McKenzie RL, Ben Liley J, Björn LO. 2009. UV radiation: balancing risks and benefits. *Photochemistry and Photobiology* 85:88–98
33. Provart NJ, Alonso J, Assmann SM, Bergmann D, Brady SM, et al. 2016. 50 years of *Arabidopsis* research: highlights and future directions. *New Phytologist* 209:921–44
34. Hancock AM, Brachi B, Faure N, Horton MW, Jarymowycz LB, et al. 2011. Adaptation to climate across the *Arabidopsis thaliana* genome. *Science* 334:83–86
35. Vogt T. 2010. Phenylpropanoid biosynthesis. *Molecular Plant* 3:2–20
36. Schilmiller AL, Stout J, Weng JK, Humphreys J, Ruegger MO, et al. 2009. Mutations in the cinnamate 4-hydroxylase gene impact metabolism, growth and development in *Arabidopsis*. *The Plant Journal* 60:771–82
37. Boerjan W, Ralph J, Baucher M. 2003. Lignin biosynthesis. *Annual Review of Plant Biology* 54:514–94
38. Lepiniec L, Debeaujon I, Routaboul JM, Baudry A, Pourcel L, et al. 2006. Genetics and biochemistry of seed flavonoids. *Annual Review of Plant Biology* 57:405–30
39. Rozema J, Boelen P, Blokker P. 2005. Depletion of stratospheric ozone over the Antarctic and Arctic: responses of plants of polar terrestrial ecosystems to enhanced UV-B, an overview. *Environmental Pollution* 137:428–42
40. Ho WC, Li D, Zhu Q, Zhang J. 2020. Phenotypic plasticity as a long-term memory easing readaptations to ancestral environments. *Science Advances* 6:eaba3388
41. Ho WC, Zhang J. 2018. Evolutionary adaptations to new environments generally reverse plastic phenotypic changes. *Nature Communications* 9:350
42. Phillimore AB, Hadfield JD, Jones OR, Smithers RJ. 2010. Differences in spawning date between populations of common frog reveal local adaptation. *Proceedings of the National Academy of Sciences of the United States of America* 107:8292–97
43. Demchik SM, Day TA. 1996. Effect of enhanced UV-B radiation of pollen quantity, quality, and seed yield in *Brassica rapa* (Brassicaceae). *American Journal of Botany* 83:573–79
44. Torabinejad J, Caldwell MM, Flint SD, Durham S. 1998. Susceptibility of pollen to UV-B radiation: an assay of 34 taxa. *American Journal of Botany* 85:360–69
45. Feng H, An L, Tan L, Hou Z, Wang X. 2000. Effect of enhanced ultraviolet-B radiation on pollen germination and tube growth of 19 taxa *in vitro*. *Environmental and Experimental Botany* 43:45–53
46. Çetinbaş-Genç A, Toksöz O, Piccini C, Kilin Ö, Sesal NC, et al. 2022. Effects of UV-B radiation on the performance, antioxidant response and protective compounds of hazelnut pollen. *Plants* 11:2574



Copyright: © 2025 by the author(s). Published by Maximum Academic Press on behalf of Hainan Yazhou Bay Seed Laboratory. This article is an open access article distributed under Creative Commons Attribution License (CC BY 4.0), visit <https://creativecommons.org/licenses/by/4.0/>.